Journal of Solid State Chemistry **166,** 369–374 (2002)
doi:10.1006/jssc.2002.9607,

Template Synthesis and Structure of a Three-Dimensional Bimetallic Phosphate

Yongnan Zhao,*[,1] Jing Ju,† Xiangming Chen,* Xiuhong Li,* Yong Wang,* Ruji Wang,‡
Ming Li,* and Zhenhong Mai*

**Institute of Physics and Center for Condensed Matter Physics, Chinese Academy of Sciences, Beijing 100080, People's Republic of China;*
†College of Chemistry and Molecular Engineering, Peking University, Beijing 100871, People's Republic of China; and ‡Department of Chemistry, Tsinghua University, Beijing 100084, People's Republic of China

Received December 13, 2001; in revised form March 27, 2002; accepted April 5, 2002

Introducing cobalt into the Zn–P–O-amine system and using oxalates as starting materials, an amine-containing open-framework zinc cobalt phosphate, $[C_2N_2H_{10}][Co_{4.2}Zn_{1.8}(PO_4)_4(HPO_4)]\cdot H_2O$ (1), has been hydrothermally synthesized. It crystallizes in monoclinic space group $C2/c$ (No. 15) with cell parameters $a = 19.214(8)$ Å, $b = 5.0152(17)$ Å, $c = 21.175(8)$ Å, $\beta = 103.06(3)^\circ$, $V = 1987.7(13)$ Å^3, $Z = 4$, $D_{cal} = 3.078\ g\ cm^{-3}$. The structure contains two sets of *M*–O–*M* linkage: *M*–O–*M* dimer and unusual infinite helical –*M*–O–*M*– chain. Connecting the dimers by phosphates leads to three-membered ring chains. The linking of the helical chains by PO_4 groups results in a sheet structure. Using the three-membered ring chains as pillars, stacking of the sheets gives rise to a three-dimensional tunnel structure. © 2002 Elsevier Science (USA)

INTRODUCTION

The synthesis and application of porous materials are an active area of solid-state chemistry due to their specific properties such as catalytic, ion exchange and intercalation. After the successful synthesis of aluminophosphates, templated metal phosphates with open-framework structures have been much studied with a view to new architectures, compositions and pore topologies (1). Since the first microporous zincophosphate with zeolite topologies reported by Stucky and co-workers (2), a great deal of effort has been devoted to the pursuit of novel structures within this system (3). Their structures consist of vertex-sharing networks of ZnO_4 and PO_4 tetrahedral, corresponding to anionic framework $[ZnPO_4^-]$, that are equivalent to those encountered in aluminosilicates of composition $[AlSiO_4^-]$. Some eye-catching results are the synthesis of a series of zincophosphates possessing 12- and 18-ring channels and very low framework densities in $N(CH_3)_4[ZnH_3(PO_4)_2]$ (4). The most excited compound is $Zn_3(PO_4)_2(PO_3OH)(H_2DACH)_2\cdot H_2O$ with hexagonal 24-ring channels (5). Another goal is to incorporate transition metal into the known phases. Transition atom incorporation has bestowed porous materials with powerful catalytic properties (6). Several new topologies have also been reported by incorporating transition species into the Al–P–O system (7). However, of the known open-framework phosphates, those of transition metals are few. Although a number of iron phosphates have been isolated (8), cobalt phosphates are seldom reported. Cobalt(II) can easily exhibit tetrahedral in addition to five- and six-coordination and cobalt doping will give rise to interesting magnetic properties and enhance the catalytic performance. This has stimulated a substantial effort to synthesize cobalt doping and pure cobalt phosphate with open-framework structures. Cobalt-doping framework structures such as alumino-, gallo- and indium phosphates have been isolated (9). Several open-framework cobalt phosphates have also been synthesized recently (10). While a number of transition-metal-doped aluminophosphates have been characterized, transition-metal-containing zincophosphates are very few (11). Our recent research is engaged in new open-framework phosphates by introducing transition metals into the Zn–P–O-amine system. With a view to bimetallic phosphate, a zinc cobalt phosphate, $[C_2N_2H_{10}]^{2+}[Co_{4.2}Zn_{1.8}(PO_4)_4(HPO_4)]\cdot H_2O$ (**1**), was hydrothermally synthesized. Here, we report its synthesis and structure.

EXPERIMENTAL SECTION

Synthesis and Initial Characterizations

Compound **1** was hydrothermally synthesized from a solution consisting of $ZnC_2O_4\cdot 2H_2O$ (0.5 g, 2.64 mmol),

---

[1] To whom all correspondence should be addressed. E-mail: zhaoyn@263.net.

0022-4596/02 $35.00

TABLE 1
Details of Data Collection, Processing, and Structure Refinement

Empirical formula	$Co_{4.2}Zn_{1.8}(PO_4)_4(HPO_4)$ $H_2O \cdot NH_3C_2H_4NH_3$
Formula weight	921.16
Temperature	295(2) K
Wavelength	0.71073 Å
Crystal system, space group	monoclinic $C2/c$ (No. 15)
Unit cell dimensions	$a = 19.214(8)$ Å, $\alpha = 90°$ $b = 5.0152(6)$ Å, $\beta = 103.06(3)°$ $c = 21.175(12)$ Å, $\gamma = 90°$
Volume	1987.7(13) Å^3
Z, calculated density	4, 3.078 g cm^{-3}
Absorption coefficient	6.076 mm^{-1}
$F(000)$	6072
Crystal size	$0.05 \times 0.10 \times 0.2$ mm^3
Theta range for data collection	1.97–27.5°
Limiting indices	$-24 < h < 1$, $-1 < k < 6$, $-26 < l < 27$
Reflections collected/unique	2990/2255
Absorption correction	Empirical
Max. and min. transmission	0.6241 and 0.1517
Refinement method	Full-matrix least squares on F^2
Goodness of fit on F^2	1.001
Final R indices $[I > 2\sigma(I)]$	$R1 = 0.381$, w$R2 = 0.0855$
R indices (all data)	$R1 = 0.0436$, w$R2 = 0.09$
Large diff. peak and hole	-0.685 and -0.868 e A^{-3}

$CoC_2O_4 \cdot 2H_2O$ (0.5 g, 2.73 mmol), H_3PO_4 (85%, 1 mL, 16.84 mmol), ethylenediamine (0.5 mL, 7.25 mmol) and H_2O (15 g, 833 mmol). The mixture with pH value of ca. 4 was heated at 170°C for 36 h in a Teflon-lined autoclave. The reaction produced blue prism crystals. Simulated X-ray patterns based on the single-crystal structure, which was in good agreement with the experimental powder X-ray data, indicate the phase purity. The zinc and cobalt contents were measured by energy-dispersive X-ray analysis. The results of three samples give an average Co/Zn value of 7 : 3. Thermogravimetric analysis (TGA) was carried out at a heating rate of 10°C min^{-1} in nitrogen. The TGA result shows two-step weight losses in the range from room temperature to 800°C. Between 300°C and 480°C all the water and ethylenediamine molecules are lost with a total loss of 10.1%, in agreement with the calculated value of 9.7%. This compound is thermally unstable. Indicated by powder X-ray diffraction, the sample becomes amorphous after calcined at 400°C for 2 h. Infrared spectra for **1**: 400–1000 cm^{-1} [ν(P–O), ν(M–O)], 1450–1650 cm^{-1} [ν(C–C), ν(C–N)], 3000–3500 cm^{-1} [ν(O–H)].

Structure Determination

A crystal with approximate dimensions of $0.2 \times 0.1 \times 0.05$ mm^3 was selected for structure determination. The room temperature (293 ± 2 K) single-crystal X-ray experiments were performed on a Bruker P4 diffractometer equipped with graphite monochromatized Mo$K\alpha$ radiation. Unit cell was refined by 27 well-centered reflections within the theta range of $4.6° < \theta < 12.5°$. Data

TABLE 2
Atomic Coordinates and Equivalent Isotropic Temperature Factors[a] (Å^2)

Atoms	x	y	z	U_{eq}	Occupancy
Co(1)	0.23829(3)	0.45026(12)	0.43221(3)	0.02780(17)	0.7
Zn(1)	0.23829(3)	0.45026(12)	0.43221(3)	0.02780(17)	0.3
Co(2)	0.23587(3)	−0.05150(13)	0.31968(3)	0.03148(18)	0.7
Zn(2)	0.23587(3)	−0.05150(13)	0.31968(3)	0.03148(18)	0.3
Co(3)	−0.00096(3)	−0.01732(11)	0.33355(3)	0.02393(16)	0.7
Zn(3)	−0.00096(3)	−0.01732(11)	0.33355(3)	0.02393(16)	0.3
P(1)	0.15046(6)	−0.0070(2)	0.43599(6)	0.0236(2)	1.0
P(2)	−0.16566(6)	−0.0150(2)	0.33137(6)	0.0252(2)	1.0
P(3)	0.02813(13)	−0.5207(4)	0.25745(12)	0.0254(5)	0.5
O(1)	0.07180(17)	0.0491(7)	0.41040(16)	0.0309(7)	1.0
O(2)	0.19484(17)	0.1109(6)	0.38946(16)	0.0309(7)	1.0
O(3)	0.16508(18)	0.6962(6)	0.44530(18)	0.0342(7)	1.0
O(4)	0.32316(17)	0.3576(7)	0.49990(16)	0.0344(8)	1.0
O(5)	−0.08814(17)	0.0511(7)	0.36345(16)	0.0303(7)	1.0
O(6)	0.28552(19)	0.6358(7)	0.36933(19)	0.0385(8)	1.0
O(7)	0.1857(2)	0.0955(8)	0.23739(18)	0.0464(10)	1.0
O(8)	0.32198(17)	0.1873(6)	0.33539(17)	0.0316(7)	1.0
O(9)	0.00045(19)	−0.3968(7)	0.30982(17)	0.0331(7)	1.0
O(10)	0.0000	−0.8222(9)	0.2500	0.0368(11)	1.0
O(11)	0.1130(3)	−0.4966(15)	0.2783(4)	0.0384(16)	0.5
O(1W)	0.1494(4)	−0.3729(18)	0.2977(4)	0.0457(19)	0.5
N(1)	−0.0931(2)	0.4642(8)	0.4500(2)	0.0328(9)	1.0
C(1)	−0.0204(3)	0.5759(10)	0.4712(2)	0.0336(10)	1.0

[a] U_{eq} defined as one-third of the trace of the orthogonalized $\mathbf{U}$ tensor.

collection was monitored by three standards every 100 reflections collected. No decay was observed except for the statistic fluctuation in the range of ±2.5%. Raw intensities were corrected for Lorentz and polarization effects and absorption by an empirical method based on Ψ-scan data.

TABLE 3
Bond Lengths (Å) and Bond Angles (deg)

M(1)–O(3)	1.937(3)	P(1)–O(3)^{a}	1.519(3)
M(1)–O(4)	1.968(3)	P(1)–O(4)^{c}	1.533(4)
M(1)–O(6)	2.002(3)	P(1)–O(2)	1.558(3)
M(1)–O(2)	2.018(3)	P(2)–O(8)^{d}	1.517(3)
M(2)–O(7)	1.937(4)	P(2)–O(7)^{e}	1.524(4)
M(2)–O(2)	1.999(3)	P(2)–O(5)	1.527(3)
M(2)–O(6)^{a}	2.005(4)	P(2)–O(6)^{d}	1.562(3)
M(2)–O(8)	2.008(3)	P(3)–O(9)	1.472(4)
M(2)–O(1W)	2.286(8)	P(3)–O(9)^{e}	1.537(4)
M(3)–O(1)	1.920(3)	P(3)–O(11)	1.594(6)
M(3)–O(5)	1.950(3)	P(3)–O(10)	1.602(5)
M(3)–O(9)	1.970(3)	N(1)–C(1)	1.478(6)
M(3)–O(10)^{b}	2.025(2)	C(1)–C(1)^{f}	1.500(10)
P(1)–O(1)	1.512(3)		
O(3)–*M*(1)–O(4)	123.71(15)	O(4)^{c}–P(1)–O(2)	104.8(2)
O(3)–*M*(1)–O(6)	104.60(14)	O(8)^{d}–P(2)–O(7)^{e}	113.7(2)
O(4)–*M*(1)–O(6)	99.71(16)	O(8)^{d}–P(2)–O(5)	109.76(19)
O(3)–*M*(1)–O(2)	111.17(15)	O(7)^{e}–P(2)–O(5)	110.9(2)
O(4)–*M*(1)–O(2)	108.56(15)	O(8)^{d}–P(2)–O(6)^{d}	109.14(19)
O(6)–*M*(1)–O(2)	107.30(14)	O(7)^{e}–P(2)–O(6)^{d}	105.3(2)
O(7)–*M*(2)–O(2)	108.09(15)	O(5)–P(2)–O(6)^{d}	107.7(2)
O(7)–*M*(2)–O(6)^{a}	148.28(16)	O(9)–P(3)–O(9)^{e}	114.4(3)
O(2)–*M*(2)–O(6)^{a}	98.71(14)	O(9)–P(3)–O(11)	106.2(3)
O(7)–*M*(2)–O(8)	98.41(17)	O(9)^{e}–P(3)–O(11)	110.8(4)
O(2)–*M*(2)–O(8)	94.72(14)	O(9)–P(3)–O(10)	107.56(19)
O(6)^{a}–*M*(2)–O(8)	95.91(14)	O(9)^{e}–P(3)–O(10)	104.40(19)
O(7)–*M*(2)–O(1W)	83.9(3)	O(11)–P(3)–O(10)	113.6(3)
O(2)–*M*(2)–O(1W)	92.7(2)	P(1)–O(1)–*M*(3)	138.5(2)
O(6)^{a}–*M*(2)–O(1W)	78.1(3)	P(1)–O(2)–*M*(2)	132.6(2)
O(8)–*M*(2)–O(1W)	171.1(2)	P(1)–O(2)–*M*(1)	105.45(18)
O(1)–*M*(3)–O(5)	102.04(14)	*M*(2)–O(2)–*M*(1)	118.88(16)
O(1)–*M*(3)–O(9)	109.55(15)	P(1)^{b}–O(3)–*M*(1)	136.4(2)
O(5)–*M*(3)–O(9)	108.37(14)	P(1)^{c}–O(4)–*M*(1)	125.7(2)
O(1)–*M*(3)–O(10)^{b}	120.53(13)	P(2)–O(5)–*M*(3)	129.8(2)
O(5)–*M*(3)–O(10)^{b}	112.12(12)	P(2)^{g}–O(6)–*M*(1)	122.2(2)
O(9)–*M*(3)–O(10)^{b}	103.91(15)	P(2)^{g}–O(6)–*M*(2)^{b}	112.3(2)
O(1)–P(1)–O(3)^{a}	111.7(2)	*M*(1)–O(6)–*M*(2)^{b}	118.60(16)
O(1)–P(1)–O(4)^{c}	109.27(19)	P(2)^{e}–O(7)–*M*(2)	133.5(2)
O(3)^{a}–P(1)–O(4)^{c}	110.5(2)	P(2)^{g}–O(8)–*M*(2)	135.3(2)
O(1)–P(1)–O(2)	110.38(19)	P(3)–O(9)–*M*(3)	128.9(2)
O(3)^{a}–P(1)–O(2)	110.01(19)	P(3)^{e}–O(9)–*M*(3)	127.2(2)
P(3)–O(10)–*M*(3)^{h}	118.20(13)	*M*(3)^{h}–O(10)–*M*(3)^{a}	122.2(2)
P(3)^{e}–O(10)–*M*(3)^{h}	116.07(13)	N(1)–C(1)–C(1)^{f}	109.8(5)

Note. Symmetry transformation codes:
$^{a}(x, -1+y, z)$.
$^{b}(x, 1+y, z)$.
$^{c}(0.5-x, 0.5-y, 1-z)$.
$^{d}(-0.5+x, -0.5+y, z)$.
$^{e}(-x, y, 0.5-z)$.
$^{f}(-x, 1-y, 1-z)$.
$^{g}(0.5+x, 0.5+y, z)$.
$^{h}(-x, -1+y, 0.5-z)$.

Direct phase determination yielded the positions of metal atoms, P and a part of oxygen atoms, and the other oxygen atoms and ethylenediamine were located in successive difference Fourier syntheses. The hydrogen atoms of ethylenediamine were generated theoretically and rided on their parent atoms in refinement. The systematic absences with $h+k$ odd for hkl, and h odd and l odd for $h0l$ suggested that the crystal belongs to space group $C2/c$ or Cc. The results of structure solution and refinement showed that there is the same disorder in both space groups so that the final structure refinement runs in space group $C2/c$. The metal positions are randomly occupied by cobalt and zinc atoms. The occupancies of these positions in final refinement were assigned as 0.7Co + 0.3Zn according to the results of refinement for occupancy and the elemental analysis by microprobe. It was found that the two-fold axis through O(10) and the midpoint of O(9) and its equivalent position $(-x,\ y,\ 0.5-z)$ lead to the phosphate group composed of P(3), O(9), O(10) and O(11) so close to the two-fold axis. The distance between P(3) and its equivalent position $(-x,\ y,\ 0.5-z)$ is only 1.055 Å, and the distance between O(11) and O(1W) is also unrealistically short (0.955 Å). On the other hand, it gave very large thermal

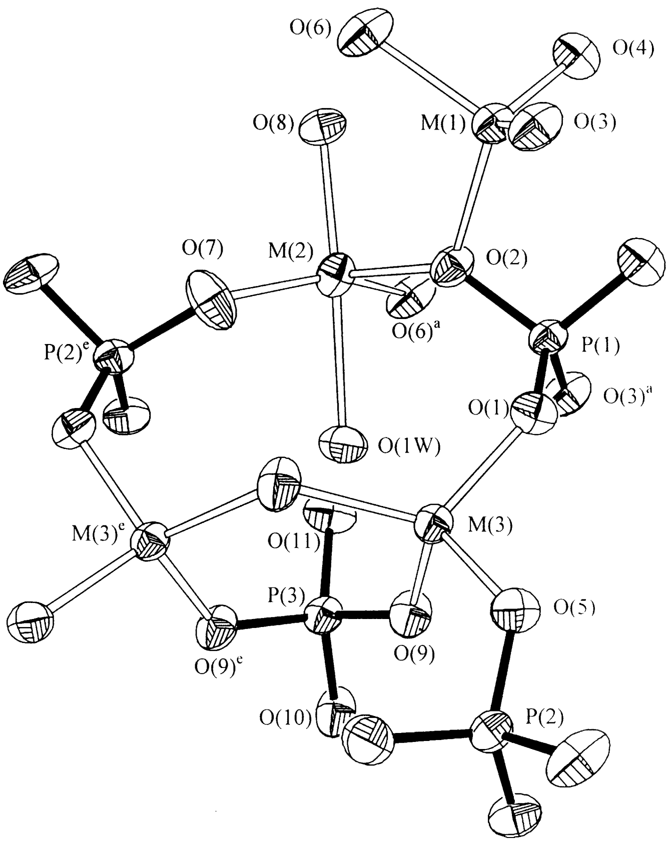

FIG. 1. ORTEP view of **1** with 50% probability ellipsoids, showing the labeling scheme.

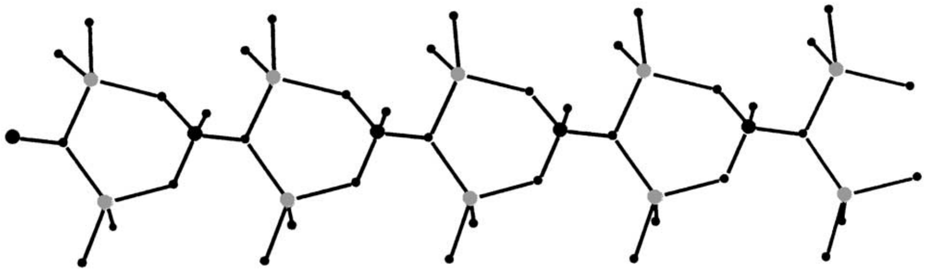

FIG. 2. Three-membered ring chains formed by linking the *M*–O–*M* dimers through PO_4 groups.

parameters for P(3), O(11) and O(1W). All the above-mentioned suggested that the two phosphate groups sharing O(9) and O(10) around the two-fold axis are alternative, and the phosphate and O(1W) in an asymmetric unit are alternative too. Therefore, the occupancies of P(3), O(11) and O(1W) were assigned to be 0.5 in the refinement. All non-hydrogen atoms were subjected to anisotropic refinement. The final full-matrix least-squares refinement on F^2 converged with $R1 = 0.0521$ and $wR2 = 0.1132$ for 2296 observed reflections $[I \geq 2\sigma(I)]$. The final difference electron density map shows no features. Details of crystal parameters, data collection and structure refinement are given in Table 1. Atom positions and selected bond lengths and angles are listed in Tables 2 and 3.

Data collection was controlled by the XSCANS program. Computations were performed using the SHELXTL NT version 5.10 program package. Analytic expressions of atomic scattering factors were employed, and anomalous dispersion corrections were incorporated.

RESULTS AND DISCUSSION

Compound **1** crystallizes in monoclinic space group $C2/c$. Its structure is comprised of an anionic coordination network with the stoichiometry $[Co_{4.2}Zn_{1.8}(PO_4)_4(HPO_4)]^{2-}$ which contains channels occupied by the diprotonated ethylenediamine and water molecules. The asymmetric unit of **1** contains 20 non-hydrogen atoms, of which 18 belong to the framework and two to the guest. Of the three unique metal atoms, *M*(1) and *M*(3) are tetrahedrally coordinated by oxygen atoms (Fig. 1). The average bond lengths of *M*(1) and *M*(3) are 1.980 and 1.966 Å with average bond angles of 109.2° for *M*(1) and 109.4° for *M*(3). The *M*(2) atom is alternatively four- and five-coordinated due to the disorder of O(1W). All three P atoms are tetrahedrally coordinated with bond lengths of 1.472(4)–1.602(5) Å and bond angles of 104.8(2)–114.4(3)°. The longest P(3)–O(10) bond length implies that O(10) is protonated, leading to the formation of HPO_4 group in compound **1**. Of the 12 oxygen atoms, O(2), O(6) and O(10) are triply bridged to the neighboring *M* and P atoms. These connections give rise to two types of *M*–O–*M* linkages in compound **1**. One is *M*(3)–O(10)–*M*(3), which is linked by PO_4 tetrahedral forming a three-membered ring chain (Fig. 2). The second is –*M*(1)–O(2)–*M*(2)–O(6)– generating an unusual infinite helical chain. These enantiotropic spirals are connected by $P(1)O_4$ and $P(2)O_4$ tetrahedrals to generate a sheet structure (Fig. 3).

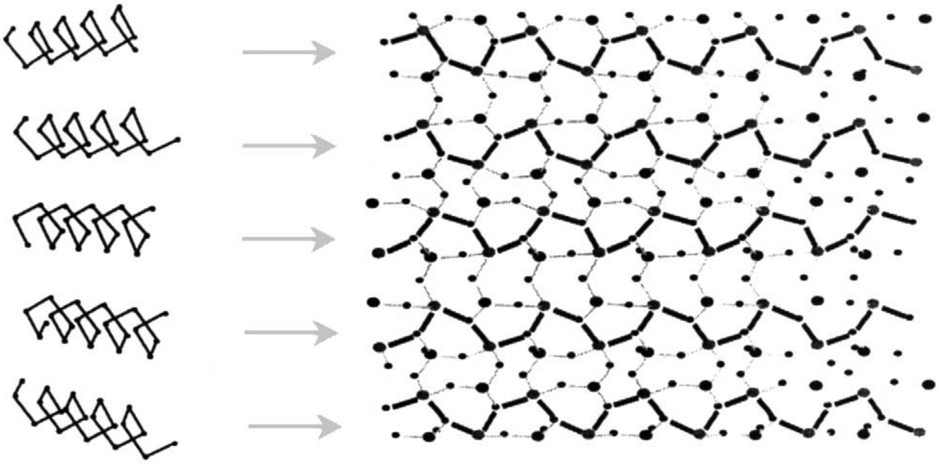

FIG. 3. Infinite helical chains (left) linked by PO_4 groups giving rise to a sheet structure (right).

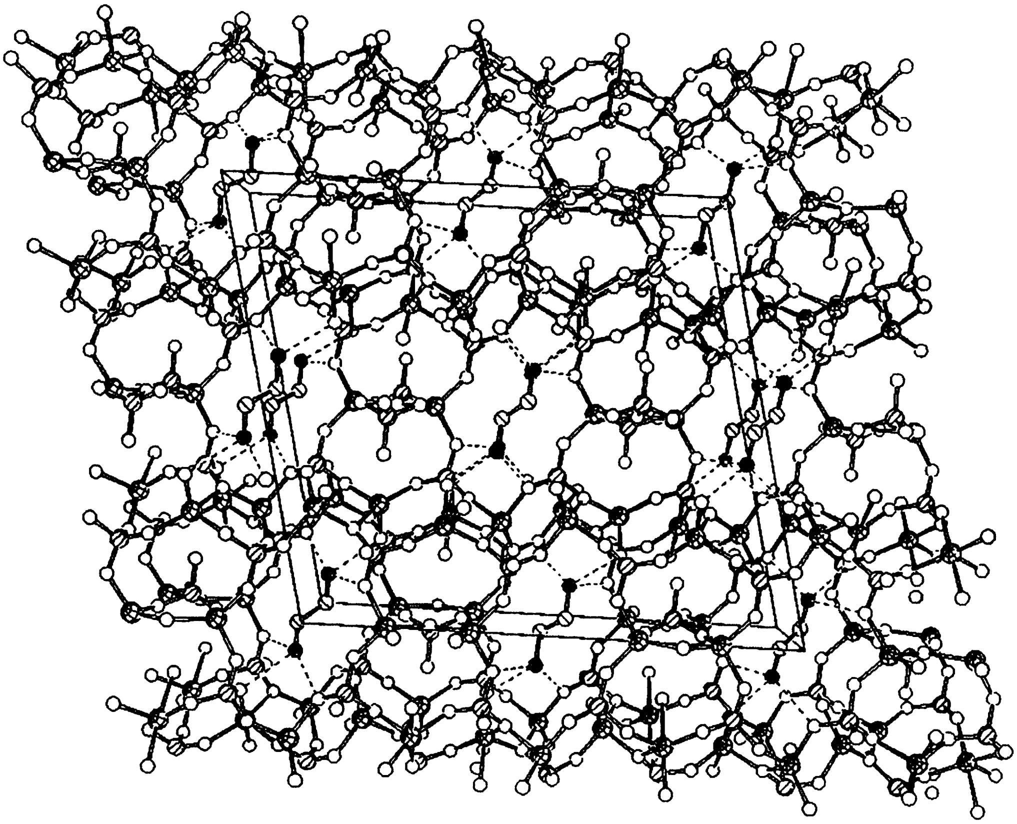

FIG. 4. View of packing plot along the *b* direction showing the six- and eight-membered ring channels with the dashed line showing the hydrogen bonds.

The three-dimensional structure of **1** can be viewed as stacking of the sheets with three-membered ring chains as pillars. The sheet is built up from the unusual infinite helical chains of –*M*–O–*M*–. These sheets are pillared by three-membered ring chains forming six- and eight-membered ring channels along the *b*-axis (Fig. 4). Viewed along the *c*-axis, the connection of MO_4 and PO_4 leads to six-membered ring channels. These six-membered ring channels can be viewed as splitting pseudo-12-membered ring channels by $P(3)O_4$ groups (Fig. 5).

The channel spaces are occupied by the amine and water molecules. The diprotonated ethylenediamine molecules are located in the eight-membered ring channels to compensate the negative framework charge. Each NH_3

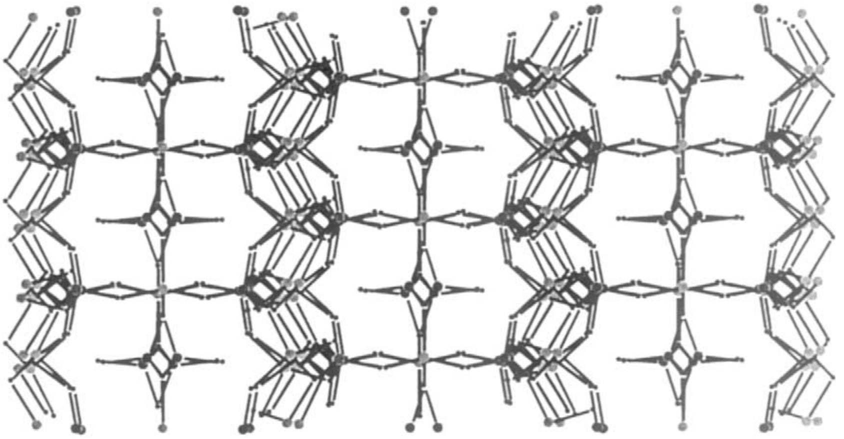

FIG. 5. Structure viewed along the *c* direction showing the six-membered ring channels.

group forms well-directed hydrogen bonds to oxygen atoms of the framework. The six-membered ring channels are occupied by the water molecules.

CONCLUSIONS

Introducing cobalt species into the Zn–P–O-amine system, a zinc cobalt phosphate has been hydrothermally synthesized using ethylenediamine as template. Structure determination shows that its structure contains two sets of *M*–O–*M* connections: *M*–O–*M* dimer and unusual infinite *M*–O–*M* helical chain. The *M*–O–*M* dimers are connected by PO_4 groups forming three-membered ring chains. The helical chains are linked by PO_4 groups, which give rise to a sheet structure. In three dimensions, the structure is constructed by sheets using three-membered ring chains as pillars forming six- and eight-membered ring channels along the *b* direction. The connection of MO_4 and PO_4 gives another six-membered channel system viewed along the *c*-axis. The protonated ethylenediamine located in eight-membered ring channels. This compound will give us further understanding on the metal phosphates and more possibilities to develop more structures in this system.

REFERENCES

1. A. K. Cheetman, G. Ferey, and T. Loiseau, *Angew. Chem. Int. Ed.* **38,** 3268 (1999) and references therein.
2. T. E. Gier and G. D. Stucky, *Nature* **349,** 508 (1991).
3. S. Neeraj and S. Natarajan, *Chem. Mater.* **12,** 2753 (2000); C. N. R. Rao, S. Natarajan, and S. Neeraj, *J. Am. Chem. Soc.* **122,** 2810 (2000); A. Choudhury, S. Natarajan, and C. N. R. Rao, *J. Solid State Chem.* **157,** 110 (2001); S. B. Harmon and S. C. Sevov, *Chem. Mater.* **10,** 3020 (1998); A. Choudhury, S. Natarajan, and C. N. R. Rao, *J. Solid State Chem.* **157,** 110 (2001); T. R. Jensen and R. G. Hazell, *Chem. Commun.* 371 (1999); C. N. R. Rao, S. Natarajan, A. Choudhury, S. Neeraj, and A. A. Ayi, *Acc. Chem. Res.* **34,** 80 (2001); Y. N. Zhao, Z. Shi, X. M. Chen, Z. H. Mai, and S. H. Feng, *Chem. Lett.* 363 (2001) and references therein.
4. W. T. A. Harrison and M. L. F. Philips, *Chem. Commun.* 2771 (1996); W. T. A. Harrison and M. L. F. Philips, *Chem. Mater.* **9,** 1837 (1997); W. T. A. Harrison and L. Hannooman, *Angew. Chem. Int. Ed. Engl.* **36,** 640 (1997).
5. G. Y. Yang and S. C. Sevov, *J. Am. Chem. Soc.* **121,** 8389 (1999).
6. J. M. Thomas and R. Raja, *Chem. Commun.* 675 (2001).
7. X. Bu, P. Feng, and G. D. Stucky, *Science* **278,** 2080 (1997); P. Feng, X. Bu, and G. D. Stucky, *Nature* **388,** 795 (1997); A. M. Chippindale, A. D. Bond, A. R. Cowley, and A. V. Poewell, *Chem. Mater.* **9,** 2830 (1997) and references therein.
8. K. H. Li, Y. F. Huang, V. Zima, C. Y. Huang, H. M. Lin, Y. C. Jiang, F. L. Liao, and S. L. Wang, *Chem. Mater.* **10,** 2599 (1998) and references therein.
9. A. M. Chippindale and R. I. Walton, *J. Chem. Soc. Chem. Commun.* 2453 (1994); A. M. Chippindale, A. R. Cowley, and R. I. Walton, *J. Mater. Chem.* **6,** 611 (1996); J. Yu, H. H.-Y. Sung, and I. D. Williams, *J. Solid State Chem.* **142,** 241 (1999).
10. P. Feng, X. Bu, S. H. Tolbert, and G. D. Stucky, *J. Am. Chem. Soc.* **119,** 2497 (1997); R. Chiang, C. Huang, C. Lin, and C. Wur, *J. Solid State Chem.* **156,** 242 (2001); A. Choudhury, S. Natarajan, and C. N. R. Rao, *J. Solid State Chem.* **155,** 62 (2000); S. Natarajan, S. Neeraj, A. Choudhury, and C. N. R. Rao, *Inorg. Chem.* **39,** 1426 (2000); S. Fernandez, J. L. Pizarro, J. L. Mesa, L. Lezama, M. I. Arriortua, and T. Rojo, *Int. J. Inorg. Mater.* **3,** 331 (2001).
11. D. Whang, N. H. Hur, and K. Kim, *Inorg. Chem.* **34,** 3363 (1995); N. Rajic, N. Logar, and V. Kaucic, *Zeolites* **15,** 672 (1995); Q. Gao, A. M. Chippindale, A. B. Cowley, J. Chen, and R. Xu, *J. Phys. Chem. B* **101,** 9940 (1997); A. N. Christensen, A. Bareges, R. B. Nielsen, R. G. Hazell, P. Norby, and J. C. Hanson, *J. Chem. Soc. Dalton Trans.* 1611 (2001).